Planta (1987) 171:145–157

Planta

Hydrodynamic radius alone governs the mobility of molecules through plasmodesmata

B.R. Terry and A.W. Robards
Department of Biology, University of York, York YO1 5DD, U.K.

Abstract. Various fluorescent molecular probes have been injected into the cytoplasm of nectary trichome cells of *Abutilon striatum* to ascertain the conductivity of the plasmodesmata. Most of the probes were based on fluorescein conjugated to a range of amino acids and peptides. The probes are not broken down by cytoplasmic enzymes during the period of observation. The results indicate that there are no specific effects of aromatic amino acids, either polar or hydrophobic types, on the conductivity of the *Abutilon* plasmodesmata, contrary to reports for other plants. The conductivity of the plasmodesmata in the trichomes is slightly greater than for any that have been studied in the tissues of other plants. It is proposed that in *Abutilon* the mobility of a probe is determined solely by the effective Stokes radius of the molecule, and that the radius of the molecule is governed by the molecular weight and, in particular, by the nature of the side groups in the peptide chain attached to the fluorochrome. Calculations are presented which indicate that channels between material in the plasmodesmatal annulus are the most likely route for the diffusion of the probes, and that the width of individual channels in the annulus is close to 3 nm.

Key words: *Abutilon* – Molecular probe, fluorescent – Nectary trichome – Plasmodesma (conductivity) – Symplastic pathway.

Introduction

It is widely believed that plasmodesmata play a critical role in the transport of water and solutes between plant cells (reviewed by Gunning and Robards 1976a) and there are increasingly frequent suggestions that they may also fulfil a regulatory function (Gunning and Robards 1976b; Olesen 1979; Erwee and Goodwin 1983; Goodwin and Erwee 1985). Nevertheless, while the animal equivalents of plasmodesmata (gap junctions) have been rigorously studied in recent years (reviewed by Pitts and Finbow 1982), detailed investigations of the transport capacity of plasmodesmata per se, in relation to the rest of the symplastic pathway, are few.

One of the major difficulties in studying the functional role of plasmodesmata is that the investigator must be sure that they are conductive in the particular tissue with which he is working. This is more likely to be so where the apoplastic pathway between cells or tissues is completely blocked and the symplastic pathway remains the only possibility for transport. Such reasoning led to the work of Clarkson and Robards (1975, 1976) who demonstrated the importance of plasmodesmata in the endodermis of cereal plant roots.

It has recently been possible to demonstrate directly the molecular continuity of plasmodesmata by using microinjected fluorescent probes. Erwee and Goodwin (1983, 1984) have used leaves of *Egeria densa* and some other plants as their test specimens, while Tucker (1982) and Tucker and Spanswick (1985) have injected dyes into the staminal hairs of *Setcreasea purpurea*. In each case the molecular exclusion limit was found to be about 700 to 800 daltons although Erwee and Goodwin (1985) have also mapped symplastic domains in *Egeria*, some of which have lower limits to conductivity. It has further been suggested (Erwee and Goodwin 1983) that group-II ions can inhibit movement of otherwise mobile fluorescent probes and that aromatic amino acids are not only relatively immobile themselves but may inhibit the movement of mobile dye conjugates.

Abbreviations: F = fluorescein; FITC = fluorescein isothiocyanate; Glu = glutamic acid; Gly = glycine; Leu = leucine; LRB = lissamine rhodamine; LYCH = lucifer yellow CH; Met = methionine; Phe = phenylalanine; Pro = proline; Ser = serine; Trp = tryptophan; Tyr = tyrosine

The method of microinjection, and the related use of microelectrodes to determine intercellular conductivity, offers such good possibilities for extending our relatively sparse knowledge of the physiological function of plasmodesmata that we have applied it to an experimental plant system which is particularly amenable to such an experimental approach, and with which we are especially familiar: namely, the secretory hairs of the *Abutilon* nectary. There are a number of advantages in using *Abutilon* for such studies: (i) The structure and physiological activity of this nectary have previously been extremely well documented and described (Findlay and Mercer 1971a, b; Findlay et al. 1971; Reed et al. 1971; Gunning and Hughes 1976; Kronestedt et al. 1986). (ii) The structure of the gland is geometrically relatively simple. (iii) It has been well demonstrated (Gunning and Hughes 1976) that an apoplastic barrier at the base of the nectary hair constrains the volume flow of prenectar to pass through the plasmodesmata between the basal cell and the stalk cell. (iv) It is possible to take thin slices of gland and to observe nectar secretion under the microscope for some hours while the trichomes continue to function normally (Findlay and Mercer 1971a). (v) The hairs make ideal subjects for microinjection in that it is possible to position micropipettes within specifically chosen, and easily observable, cells. Further, injections into adjacent cells are also experimentally straightforward. (vi) Clonal material can be propagated so that it that will flower all the year round.

The results reported in this paper represent our initial studies of the *Abutilon* system. It has been necessary to determine the molecular exclusion limits to intercellular conductivity and to compare them with the data provided by the authors referred to above. We have made an assessment of the factors controlling intercellular movement based not simply on the molecular weight of the dye conjugates but also by taking into account the shape and effective Stokes radius of the molecules. Using such methods, it is then possible to predict the minimum size of the channel that must support intercellular movement. The discussion as to whether plasmodesmata allow intercellular communication through *either* the desmotubule *and-or* the cytoplasmic annulus remains unresolved. Overall et al. (1982) have forwarded convincing arguments that, in *Azolla* roots, the desmotubule is a solid rod and communication can only be via the cytoplasmic annulus. A functionally similar model has been suggested by Thomson and Platt-Aloia (1985) for the salt glands of *Tamarix*. It is already known that the trichome plasmodesmata of *Abutilon* have a relatively wide cytoplasmic annulus (Gunning and Hughes 1976) compared with that of many other plants (for a review, see Robards 1975). Determination of the effective limiting dimensions of microinjected dyes should allow the resolution of this problem, at least for *Abutilon*.

Material and methods

Plant material. Plants of *Abutilon striatum* Dicks (*A. thompsonii* André) were grown from cuttings in heated greenhouses. A regime of 16 h light, 8 h dark and a minimum temperature of about 17° C ensured that the plants produced flowers all year round. Large quantities of nectar are secreted by mature flowers from specialised trichomes borne on the inner face of the sepal's base. Mature, secreting trichomes from open flowers and immature, non-secreting trichomes from closed buds were used in the experiments. It was thought that changes in the molecular conductivity of the plasmodesmata might occur with the onset of secretion. Vertical slices of nectary tissue, about 100 µm thick, were cut under distilled water then transferred to a transparent injection bath, filled with 1.5 mM KCl (Fig. 1). The tissue slices were held in place against the thin base of the bath by an elastic nylon mesh in such a way that the trichomes were freely accessible for injection.

Dyes and conjugates. Most of the molecular probes were conjugates of fluorescein isothiocyanate (FITC) and various amino acids or oligopeptides. These conjugates were made essentially as described by Simpson (1978). Peptides of the glycine series $(Gly)_8$ to $(Gly)_{12}$ were synthesised by a solid-phase method (Merrifield 1964). N-t-butoxycarbonyl glycine used in the process was obtained from Aldrich Chemical Co., Gillingham, Dorset, UK. All other amino acids and peptides were obtained from Sigma Chemical Co., Poole, Dorset, UK, as was the FITC (isomer 1). Conjugates were purified either by descending paper chromatography using 50 mM $KHCO_3$ as solvent, or by thin-layer chromatography (TLC) on Kieselgel 60 G plates (Merck, Darmstadt, FRG) using organic solvents. Ethyl ethanoate + 2% or 6% acetic acid gave good separation of most of the conjugates, but probes in the glycine series were best separated by a 1:1:1:1 mixture of butanol, ethanoic acid, ethyl ethanoate and water. Purified probes were dried and stored at −20° C. The purity of each probe was checked by TLC before it was injected. Lissamine rhodamine (LRB; Gurr, BDH Chemicals, Poole, UK), FITC-labelled dextran (MW 18900) and lucifer yellow CH (LYCH; Sigma) were also used as molecular probes. Lissamine rhodamine was filtered through acid-washed activated charcoal before use. Probes were prepared as approx. 1 mM solutions in 5 mM $KHCO_3$ (pH 8). The solutions were filtered through 0.22-µm Millipore filters (Millipore S.A., France) prior to injection. At pH 8 all the probes used were negatively charged.

Stability of the probes in cytoplasm. Enzyme extracts were prepared by grinding four nectaries, excised from underlying sepal tissue, with a little acid-washed sand in 4–5 ml of ice-cold 0.05 M 2-amino-2-(hydroxymethyl)-1,3-propanediol (Tris)-HCl buffer, pH 8.5, which also contained 1 mM dithiothreitol and 400 mM sucrose (being the approx. sugar concentration to which the cytoplasm of the trichome cells would normally be exposed). Aliquots of the molecular probes (approx. 10 mM) were incubated with the extract at volume ratios of 1:1, 1:2 and 2:1 at 37° C for 30 min. The samples were then freeze dried, the fluorochromes extracted with methanol and exam-

ined for breakdown by TLC on Kieselgel 60 alufol plates. The extracts were assayed for protein concentration and the activities of hexokinase and acid phosphatase. Hexokinase activity was measured by the production of glucose-6-phosphate at pH 8.5 as shown by the reduction of NADP by glucose-6-phosphate dehydrogenase. Acid-phosphatase activity was assayed at pH 4.8 using a standard *p*-nitrophenol phosphate method.

Electrophysiology and iontophoresis. The molecular probes were injected into the cells by iontophoresis from single-barreled micropipettes. The micropipettes were pulled from 1-mm filamented aluminosilicate capillaries (Clark Electromedical Instruments, Pangbourne, Berks., UK). Tip diameters of <0.5 µm (40–70 MΩ, backfilled with 100 mM KCl) were achieved on a slightly modified horizontal electrode puller (C.E. Palmer Ltd., London). The strength of the aluminosilicate glass is needed to prolong the life of the micropipettes since the cuticle and wall of a trichome cell form a particularly tough barrier. The tip of each micropipette was backfilled with a small volume of the chosen molecular-probe solution, the remaining volume being filled with 100 mM KCl solution. Each micropipette was sealed to a homemade Ag/AgCl half-cell, also filled with 100 mM KCl, and connected via the appropriate probe to either the iontophoresis or electrometer module in a WPI S7000 mainframe unit (WPI Inc., Newhaven, Conn. USA). The microelectrode was held in a Huxley-Goodfellow 3000 micromanipulator (Goodfellow Metals, Cambridge, UK). An agar salt bridge to a second Ag/AgCl half-cell took the bathing medium to earth. The impedance of filled micropipettes was typically about 100 MΩ.

Probes were generally injected into the tip cells of trichomes as these were the most easily accessible. Penetration of a cell was monitored by the potential at the micropipette tip. Steady potentials of -60 to -70 mV indicated that the glass tip had penetrated into the cytoplasm of the trichome cell. To expel the probe molecules into the cytoplasm the electrode potential was made more negative. A current of between -1.5 and -3 nA for 10 s was usually sufficient to inject enough dye into the cells for observations to be made. Some conjugates were particularly difficult to eject and required higher currents in square-wave pulses of 1 s duration alternated with positive current pulses to unblock the microelectrode's tip. Transport numbers for most of the probes were in the range 0.01 to 0.001. Membrane potentials of injected cells were monitored before and after iontophoresis and used as an index of the integrity of the cell throughout the period of observation. Results were discarded if iontophoresis produced significant permanent changes in the cell membrane potentials.

Microscopy. All injections and observations were made on the stage of an inverted microscope (Diaphot, Nikon, Tokyo, Japan) fitted with epi-fluorescence optics, at a total magnification of X400 (Nikon CF Achromat LWD 40 × C objective, N.A. 0.55). The blue excitation cassette (420–485 nm excitation, 510 nm dichroic mirror and 520 nm emission filters) gave good intensities of fluorescence with all the probes used. When co-injected, the orange fluorescence of LRB was easily distinguished from the bright green fluorescence of FITC conjugates with this one filter setting. Exposure of the probes to the excitation light was kept to a minimum to prevent bleaching. The microscope ws fitted with a 35-mm camera (Olympus OM2). Images were recorded on Kodak (Hemel Hemsted, Herts., UK) Tri-X or Ektachrome 200 (daylight) film.

Assessment of movement. Mobilities have been expressed as the percentage of injections of a particular probe which showed movement from the cytoplasm of the injected cell to the cytoplasm of the next cell and so on down the trichome. A time limit of 60 s for the fluorochrome to reach the threshold of detection in the first adjacent cell was imposed to standardise the assessment. Within 60 s a mobile probe would have been detectable in the adjacent cell, a non-mobile probe would not. Subsequent measurements with a microfluorimeter (Leitz Diavert with MPV photometer; Leitz, Wetzlar, FRG) showed that the probes reached a concentration of about 50 µM in the tip cells, and that the minimum detectable level of probe in adjacent cytoplasm would have to be about 1 µM in order to be seen above the level of autofluorescence from the trichome cuticle.

For each injection the probe tip could be located in the subcuticular space, the space between wall and cell membrane, the cell vacuolar system or in the cytoplasm. In some instances the electrode potential was not sufficient to distinguish between these different compartments. However the spread of fluorescence from the site of injection, and the texture of the fluorescent image distinguished cytoplasmic injections from all others (see Figs. 2–5). A minimum of 15 cytoplasmic injections was performed for each probe to assess mobility. None of the fluorescent probes showed any ability to permeate plasmamembranes, nor indeed the tonoplasts of trichome cells.

Results

Stability of the probes. The nectary extract used for the lysis experiments contained 0.47 $mg \cdot ml^{-1}$ protein as determined by a BioRad microassay against bovine serum albumin standards; the specific activity for hexokinase (at pH 8.5) was 0.179 $U \cdot mg^{-1}$ protein, and for acid phosphatase (at pH 4.8) was 0.05 $U \cdot mg^{-1}$ protein. Although the extract clearly contained considerable quantities of vacuolar enzymes, it also showed a high hexokinase activity which indicates that cytoplasmic enzymes were also extracted well. The enzyme incubations were carried out at pH 8.5 to reduce the activity of the acid phosphatases and to mimic more accurately the conditions likely to be encountered by the probes when they were injected into the cytoplasm. None of the incubations showed any evidence that the probes were broken down by enzymes in the extract (30 min at 37° C). It therefore seems likely that the probes remain intact in the environment of the cytoplasm, at least during the few minutes of observation. This result is in agreement with the findings of other workers (Tucker 1982; Goodwin 1983).

Mobility. Each result in Table 1 shows the probability that a particular probe will move or not when injected into a trichome cell. The probability is not a direct measure of the rate of movement of a probe. If an injection were to lead to movement, the amount of probe required for detection (1 µM) would normally have accumulated in the adjacent cell after 10–15 s (Fig. 2). Some conjugates were occasionally reluctant to iontophorese from the micropipette tip, and thus the concentration of

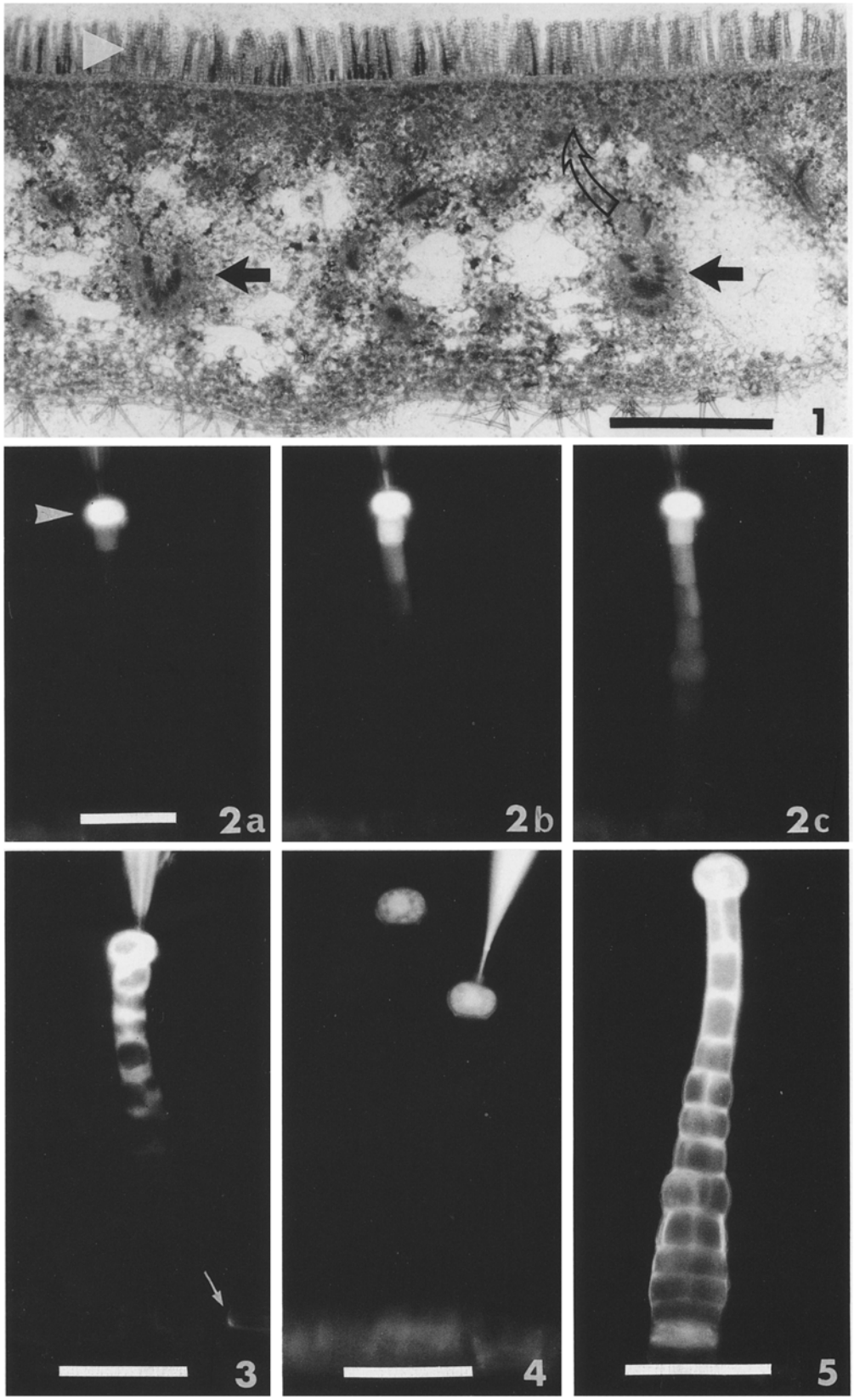

Figs. 1–5. Micrographs of the *Abutilon* nectary and nectary trichomes. **Figs. 2–5** are fluorescence micrographs

Table 1. Mobilities of molecular probes through the nectary trichomes of *Abutilon striatum* var. Thompsonii, expressed as the percent of injections which show movement of the probe, judged 60 s after injection. Figures in brackets are for immature, non-secreting trichomes (from flower buds 2.5 to 3.0 cm long). All other values are for mature trichomes. The value of net charge on a probe is for pH 8

Probe	MW (Da)	Mobility (% of inj.)	Charge
Fluorescein	376	90	−2
LRB	476	100	−2
LYCH	457	100	−2
F-Glu	536	95	−3
F-$(Leu)_3$	747	80 (80)	−2
F-Gly	464	100	−2
F-$(Gly)_3$	578	100	−2
F-$(Gly)_5$	692	100	−2
F-$(Gly)_6$	749	80	−2
F-$(Gly)_8$	862	75	−2
F-$(Gly)_9$	919	75	−2
F-$(Gly)_{10}$	976	75	−2
F-$(Gly)_{12}$	1090	70	−2
F-Phe	555	75	−2
F-Met-Phe	685	80 (80)	−2
F-Ser-Phe	641	70 (85)	−2
F-Gly-Phe	612	60 (55)	−2
F-Pro-Phe	651	30 (50)	−2
F-Trp-Phe	739	5 (10)	−2
F-Trp	593	20 (15)	−2
F-$(Trp)_2$	779	25 (20)	−2
F-Trp-Leu	705	40 (10)	−2
F-$(Phe)_4$	996	100 (65)	−2
F-$(Tyr)_3$	897	20 (10)	−2
F-Dextran	19000	0	−2

probe in the injected cell was slow to build up: if the effective concentration of probe in the injected cell did not reach about 100 μM within the 10 s of iontophoresis, the result was discarded.

Molecular probes were injected into mature secreting trichomes as well as into trichomes taken from unopen buds which, while they looked structurally similar, were at least 2 d from the start of their secretion phase. The immature trichomes were characterised by a much less obviously vacuolated cytoplasm and the adherence of their cuticles to the cell walls. This study has not revealed any significant difference in the conductivity of plasmodesmata in mature and immature trichomes, indicating that it is unlikely that great changes in conductivity occur with the onset of nectar secretion.

Membrane potentials returned to their normal values (−60 to −80 mV) within 1–5 s after the hyperpolarisation caused during the injection of the probes. The potentials were maintained for long periods (some were monitored for over 1 h) which indicates that neither the procedure nor the probes caused much damage to the integrity of the cell, at least while the micropipette was in position. Trichome cells do not exhibit cytoplasmic streaming, so this indicator of metabolic integrity cannot be used in situ, however it should be noted that even small concentrations (<10 μM) of mobile or non-mobile probes injected into the cytoplasm of *Tradescantia purpurea* staminal hair cells

Fig. 1. A freehand vertical section through the sepal of a secreting *Abutilon* flower to show the location of the nectary trichomes (*white arrowhead*). The major veins (*black arrows*), 500 μm from the trichomes, supply prenectar via minor vessels to the dense parenchyma which lies below the trichomes. The prenectar can enter a trichome only via the proximal wall of its basal cell; other routes into the trichome are blocked by an apoplastic barrier similar to the casparian band found in root endodermal cells. Mature trichomes on a slice of tissue of the thickness shown will continue to secrete nectar for several hours. × 50; bar = 500 μm

Fig. 2a–c. A single immature trichome photographed at 30-s intervals. The mobile probe F-Glu has been injected into the tip cell (*arrowhead*) and can be seen to diffuse rapidly through the cytoplasm of the trichome. Note the smooth appearance of the cytoplasmic distribution of fluorochrome which is characteristic of injections into young, non-vacuolated trichome cells. Time after injection: **a** 15 s, **b** 45 s, **c** 75 s. × 300; bar = 50 μm

Fig. 3. A mature and secreting trichome injected with F-$(Gly)_3$. The uneven distribution of the fluorochrome within each cell confirms that the probe is in the cytoplasmic compartment. The trichome cells develop larger vacuoles as they mature. A small amount of autofluorescence can be seen from the cuticle which covers the trichomes. The apoplastic barrier in the radial walls of the stalk cell and basal cell of each trichome also autofluoresces quite strongly (*arrow*). × 400; bar = 50 μm

Fig. 4. The tip cells of two immature trichomes have been injected with F-Trp-Phe. No diffusion of the probe into the adjacent cells is detectable 60 s after injection. The probe is classed as immobile for these two injections. × 400; bar = 50 μm

Fig. 5. The anatomy of a trichome as revealed by the spread of fluorochrome throughout the spaces which lie between the cuticle and the cell walls of the trichome. All the probes used will spread in this way if they enter the subcuticular space; however, the texture of the fluorescent image is very different from that seen when the probes are located in the cytoplasm, thus the two types of injection can be distinguished easily. × 450; bar = 50 μm

Table 2. Dimensions of the molecular probes derived from space-filling models. Unit dimensions represent the size of the fluorochrome or the peptide tail alone. Conjugate dimensions are the values for the most likely conformation of each entire molecule, and include allowances for hydration shells. Double rows of figures indicate that a molecule tapers along its length, and show width and depth values for both ends

Molecular probe	Dimensions L:W:D (nm)		Comments
	Unit	Conjugate	
FITC	1.20; 1.35; 0.80	1.40; 1.70; 1.20	Tetrahedron
LRB	1.20; 1.55; 0.80	1.40; 2.00; 1.20	Tetrahedron
LYCH	1.35; 1.35; 0.40	1.80; 1.70; 0.80	Planar
F-Gly	0.55; 0.55; 0.45	2.10; 1.70; 1.20 0.60; 0.80	Taper to Tail
F-$(Gly)_3$	0.60; 1.00; 0.45	2.10; 1.70; 1.20 1.10; 0.80	Random coil
F-$(Gly)_5$	1.50; 0.85; 0.95	3.10; 1.70; 1.20 1.10; 1.00	Random coil
F-$(Gly)_6$	1.90; 0.85; 0.95	3.50; 1.70; 1.20 1.10; 1.00	Random coil
F-$(Gly)_{12}$	2.40; 1.20; 0.95	4.00; 1.70; 1.20 1.20; 1.00	Random coil
F-$(Leu)_3$	1.50; 1.10; 0.55	3.10; 1.70; 1.20 1.20; 0.80	Side groups together behind F head
F-Glu	0.85; 0.80; 0.55	2.40; 1.70; 1.20 1.00; 0.80	Carboxyls out from F
F-Phe	0.90; 0.65; 0.55	1.40; 1.70; 1.40	Folded back onto F
F-Met-Phe	1.20; 1.10; 0.55	1.45; 1.70; 1.30	Folded back onto F
F-Ser-Phe	1.00; 1.15; 0.65	1.65; 1.70; 1.40	Folded back onto F
F-Gly-Phe	0.90; 1.00; 0.55	1.65; 1.70; 1.40	Folded back onto F
F-Pro-Phe	0.90; 1.25; 0.70	1.75; 1.75; 1.45	Folded back onto F
F-Trp-Phe	0.85; 1.15; 0.75	1.80; 1.80; 1.80	Folded back onto F
F-Trp	0.65; 1.15; 0.80	1.60; 1.75; 1.60	Folded back onto F
F-$(Trp)_2$	0.95; 1.15; 0.80	1.70; 1.75; 1.60	Folded back onto F
F-Trp-Leu	0.80; 1.15; 0.80	1.60; 1.75; 1.50	Folded back onto F
F-$(Phe)_4$	1.75; 1.00; 0.70	3.35; 1.70; 1.20 1.40; 1.00	Phe rings together out from F
F-$(Tyr)_3$	1.40; 1.15; 0.70	3.00; 1.70; 1.20 2.30; 1.10	Tyr rings alternate out from F
F-Dextran (MW 19000)	Stokes radius 3.20		Calc. Granath and Kvist (1967)

caused an abrupt, if temporary, halt in the streaming; penetration by the micropipette and injection of $KHCO_3$ had no effect on the same cytoplasmic streaming. A series of co-injections of mobile LRB and the least mobile conjugate, F-Trp-Phe, were performed to determine whether the presence of an immobile probe affected the conductivity of the plasmodesmata: the mobility of LRB was not appreciably affected by the presence of F-Trp-Phe. Co-injection of the free peptide Trp-Phe with LYCH (10 mM and 2 mM respectively in the probe tip) had no effect on the mobility of the LYCH. Thus there is no evidence to indicate that the injection of probes, mobile or non-mobile, causes any permanent changes within the cells during the course of observation which might lead to changes in the usual conductivity of the plasmodesmata.

The mobility figures can be taken to represent the percentage of trichomes in the flower which

have plasmodesmata of sufficient aperture to allow passage of a particular probe. Mobilities have all been rounded to the nearest 5%, and represent the results of cytoplasmic injections only. About 30% of all injections into mature trichomes were vacuolar penetrations, and only about 5% with immature trichomes. Probes injected into the vacuole system do not appear to be able to get out into the cytoplasm nor pass from one cell to the other unless the vacuole is ruptured. Not even LRB or LYCH could escape the confines of the vacuole. Withdrawal of the micropipette usually caused the release of some cytoplasm, but many of the cells resealed and in these the probes stayed in, unable to diffuse through the plasma membrane. Eventually the fluorescence would become distributed throughout the entire trichome. Interestingly, no probe, not even the highly mobile LYCH, was ever observed to pass from the basal cell of a trichome into any cell of the underlying sepal tissue. Presumably there is a tightly controlled symplastic barrier between the nectary cells and the trichome (there are over 10 plasmodesmata $\cdot \mu m^{-2}$ to permit symplastic transport between basal cells and nectary cells). Similar symplastic barriers or domains have been reported by Erwee and Goodwin (1985) in *Egeria densa*.

Estimates for the likely dimensions of the probe molecules were made from space-filling models (Fig. 6). The values shown in Table 2 are for the box dimensions needed to enclose the molecules completely. The FITC molecule is tetrahedral, consists of three mildly polar aromatic rings and has the isothiocyanate group attached to one of the vertices. The isothiocyanate group forms a thiourea link with an amino group to attach peptides or amino acids to the FITC head. This link allows considerable rotation about two covalent bonds separated by approx. 109°. Because of this, and because of the hydrophobic nature of parts of the FITC head, a large number of conformations are possible for some of the conjugates, especially those which contain the hydrophobic aliphatic and aromatic side groups which might be expected to fold back around the FITC molecule. Table 2 contains values for the sizes of the fluorochromes, for the amino acids and peptides in various conformations and for the most likely dimensions of the complete conjugates plus their hydration shells, assuming an hydrophilic environment.

Discussion

The conductivity of plasmodesmata in the nectary trichomes of *Abutilon* is different in several respects from the conductivities reported for the plasmodesmata in *Setcreasea purpurea* staminal hairs, in the leaf mesophyll cells of *Elodea* and in the leaf epidermal cells, and cells of other domains, of *Egeria densa*. For comparison, F-$(Leu)_3$ MW 747 is immobile in *Setcreasea* but shows 100% mobility in *Abutilon*; F-$(Gly)_6$ MW 749, is immobile in *Egeria* leaf cells and has a markedly reduced mobility in *Elodea* mesophyll but is 80% mobile in *Abutilon*, and at a molecular weight greater than any of the limits listed above, F-$(Gly)_{12}$ MW 1090 is still mobile (70%) in *Abutilon*.

Aromatic amino acids do not appear to affect the mobilities of molecular probes through *Abutilon* plasmodesmata in the way reported in other plants. Tucker (1982) and Erwee and Goodwin (1984) showed that fluorescent probes which included aromatic amino acids in their peptide tails could not pass through the plasmodesmata being investigated. Erwee and Goodwin further reported that the presence of an aromatic amino acid, whether part of the probe or injected separately, reduced or even prevented the movement of otherwise freely mobile probes. The aromatic side groups apparently had a direct effect on the conductivity of the plasmodesmata. No such dramatic effects were observed in *Abutilon*.

Probes which could not move through the *Abutilon* trichomes did not appear to have any direct effect on the conductivity of the plasmodesmata. When F-Trp-Phe was co-injected with LRB, in approximately equal concentrations, it had no significant effect on the movement of the mobile probe. Neither did free aromatic amino acids appear to reduce the conductivity of the plasmodesmata: the peptide Trp-Phe had no effect on the spread of LYCH when co-injected (but in these co-injections it was impossible to say just how much peptide was injected with the LYCH). Perhaps none of this is unexpected since the fluorochromes themselves are composed of aromatic rings and yet are freely mobile in their unconjugated forms; it would be strange if an aromatic peptide had some particular effect on plasmodesmatal conductance but that fluorescein or LYCH did not. Neither polar rings (e.g. of the fluorochromes) nor hydrophobic rings (e.g. of phenylalanine) appear to have any effect on the conductivity of the plasmodesmata in *Abutilon* nectary trichomes. It is possible that the plasmodesmata of other plants are more sensitive to the influences of certain aromatic groups than are those of *Abutilon*. It is also possible that the only effect that the aromatic groups have is on the size of the probe molecule, and that this might explain most of the results found for other plants.

Any hypothesis designed to predict the likely mobility of a molecular probe through the plasmodesmata of the *Abutilon* trichomes should take into account the following observations:

1) Probes with polar aromatic residues are less mobile than probes of similar MW but which have exclusively hydrophobic aromatic residues: – F-$(Tyr)_3$ is less mobile than F-$(Phe)_4$.

2) The larger the aromatic side group, the less mobile is the probe: – F-Trp is less mobile than F-Phe.

3) Addition of a non-aromatic amino acid to the amino terminus of phenylalanine decreases the mobility of the resulting probe, as compared to F-Phe or an aliphatic type probe of similar molecular weight such as F-$(Gly)_5$ or F-$(Leu)_3$; so, F-Gly-Phe, F-Ser-Phe, F-Pro-Phe are less mobile than F-Phe, F-$(Gly)_5$ or F-$(Leu)_3$.

4) Addition of leucine, an aliphatic non-polar residue, to the carboxyl terminus of tryptophan increases the mobility slightly; addition of phenylalanine at the same position decreases the mobility. Thus F-Trp-Phe is less mobile than F-Trp, but F-Trp is less mobile than F-Trp-Leu.

It is proposed that the mobility of these molecular probes can be explained simply in terms of their effective Stokes radii.

Composition of the conjugates and their sizes. Space-filling models allow a good estimate of a molecule's dimensions to be made and they can indicate which conformations are most energetically favourable and therefore which are the most probable. The dimensions given in Table 2 are derived from space-filling models.

Amino acids can be divided into three classes on the basis of their hydrophobicity: a hydrophobic class which includes leucine, methionine, phenylalanine and tryptophan; a moderately polar class which includes glycine, serine and tyrosine and a very polar class of which proline and glutamic acid are members (Rose et al. 1985). The degree of hydrophobicity of residues and their distribution within the peptide is the main factor which determines the conformation adopted by the molecule. Conjugates which contain a terminal phenylalanine will amost certainly have the peptide tail twisted back over the fluorescein moiety so that the hydrophobic ring of the amino acid can lie next to the aromatic rings of the fluorochrome, and be effectively hidden from the solution (Fig. 6b, e, f, g). The free-energy change associated with such a conformation will tend to stabilise the spherical structure. If a more polar residue is inserted between the fluorescein and the Phe moieties, it will tend to increase the radius of the molecule due to the attractive forces from the surrounding hydration shells (cf. Fig. 6b and 6f). For the following conjugates the order of decreasing size should be: F-Pro-Phe, F-Gly-Phe/F-Ser-Phe, F-Met-Phe, F-Phe, which is very similar to the order of increasing mobility for the conjugates. The aromatic group of tryptophan is uncomfortably big to fit easily against the fluorescein rings; the conjugate can be expected to be substantially larger than F-Phe. F-Trp-Phe (Fig. 6g) will be larger still as the phenylalanine residue takes up position against the fluorescein rings. Leucine does not decrease the mobility of F-Trp-Leu relative to F-Trp. It is possible that the leucine residue, with its free terminal carboxyl group, is not strongly attracted to the fluorescein moiety and thus does not contribute significantly to the overall Stokes radius. The large peptides of F-$(Phe)_4$ and F-$(Tyr)_3$ seem to be too big (from models) to wrap around the fluorescein; Figs. 6c and 6 h show more likely conformations. In F-$(Phe)_4$ the rings are stacked together by the combined forces of mutual tatraction and hydrophobic repulsion. The rings of tyrosine, being more polar, will tend to be opened out by hydration shells, and the whole molecule will be wider and almost as long as F-$(Phe)_4$ even though it contains one less amino acid. It is difficult to ascribe an effective Stokes radius to most of the molecular probes since, as can be appreciated from Table 2, many are far removed from a spherical conformation. However, F-Gly-Phe, F-Pro-Phe, F-Trp and F-Trp-Phe are probably nearly spherical, and their mobility figures indicate that a Stokes radius of about 0.9 nm (F-Trp-Phe) approaches the molecular exclusion limit for the *Abutilon* plasmodesmata (subject to the criteria for deciding mobility).

Rate of diffusion versus radius of permeant. Relatively small changes in the Stokes radii can cause large differences in the mobilities of molecular probes, particularly if the pores through which the diffusion takes place are close to the size of the permeant molecules. If we consider the diffusion of a fluorescent probe from the tip cell (T) into the first (adjacent) column cell (C), the kinetics can be described by:

$$1 - X = \exp(-kt) \quad (1)$$

where X is the ratio of concentration of fluorescent probe C:T, and k is the rate constant for diffusional filling. The assumptions are that: the equilibrium concentrations in C and T will be equal; cytoplasmic diffusion will be non-limiting; the dwell time in the pores will be short relative to the total diffusion time; the probe does not move

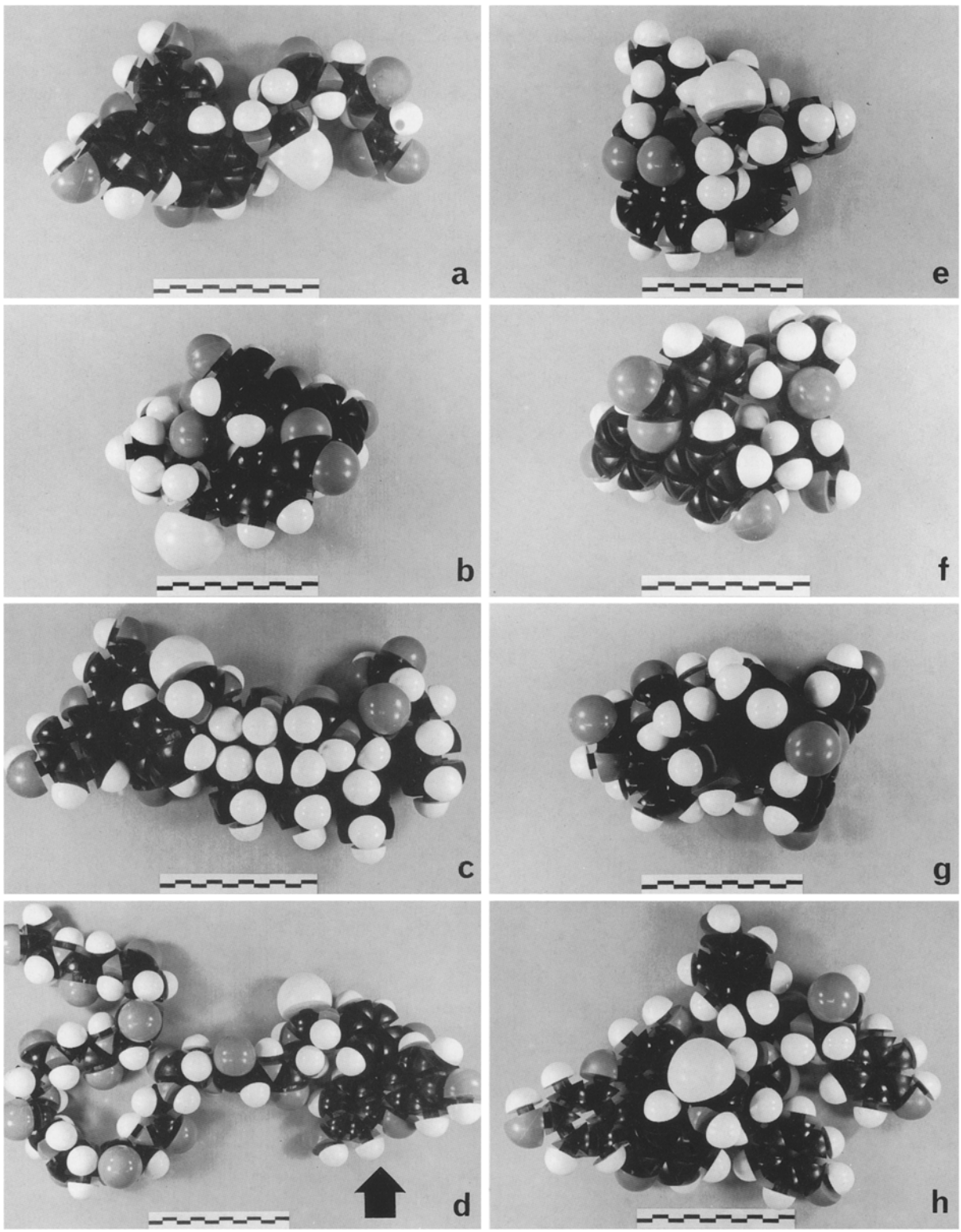

Fig. 6a–h. Space-filling models of some of the FITC-peptide probe molecules. The molecules depicted in **a–d** are freely mobile through the plasmodesmata of *Abutilon* nectary trichomes, those in **e–h** are much less mobile (see Table 1). The molecules are as follows: **a)** F-$(Gly)_3$, **b)** F-Met-Phe, **c)** F-$(Phe)_4$, **d)** F-$(Gly)_{12}$, **e)** F-Trp-Leu, **f)** F-Pro-Phe, **g)** F-Trp-Phe, **h)** F-$(Tyr)_3$. The F moiety (*arrowed* in **d**) has a tetrahedral shape and consists of three linked aromatic rings. The peptide chains attach to the F group by a thiourea bond which allows considerable freedom of movement. Chains with neutral or polar side groups will extend away from the F group into the aqueous environment (**a, d, h**); those with hydrophobic side groups will fold back onto the relatively hydrophobic surface of the F moiety (e.g. **b, e, f, g**). It should be noted that the depth of the molecules is not easily appreciated from these figures; Table 2 contains values for the dimensions of the molecules depicted (with allowances for hydration shells). All marker bars = 1 nm

from C to the next adjacent column cell in significant quantities during the period of measurement. These assumptions are valid for probes close to the limits of mobility.

$$k = PA/V \quad (2)$$

where A is the area of the interface across which diffusion takes place, P is the permeability coefficient of that interface and V is the volume of C.

Since diffusion can only occur through the plasmodesmata, length d, the patent area of each pore, p, can be found from:

$$p = (kVd)/ND' \quad (3)$$

(Paine et al. 1975) where D'/d, D' being the translational diffusion coefficient of the probe in the pore, substitutes for the coefficient P in eqn. (2), and N is the total number of pores in the interface. For a probe which just reaches the limit of detection in C (1 μM) after 60 s, from a concentration of 50 μM in T, a minimum value of k can be calculated, and from that a minimum value of p.

From eqn. (1), $k_{min} = 3.367 \times 10^{-4}$.

From anatomical measurements, $V = 1.5 \cdot 10^{-16}$ m^3, $d = 5 \cdot 10^{-7}$ m, and $N = 400$ plasmodesmata. D' is assumed to be the same as the cytoplasmic translational diffusion coefficient, and is estimated to be about $4.0 \cdot 10^{-11}$ $m^2 \cdot s^{-1}$ (extrapolated from Paine et al. 1975 for a molecule of Stokes radius 1.0 nm). Then from (2), $p_{min} = 1.578 \cdot 10^{-18}$ m^2.

Figure 7, redrawn from Paine et al. (1975) gives the relationship between the radius, r, of a cylindrical pore and the apparent area, p, available for diffusion for a molecule of Stokes radius a. The curves were generated from;

$$p = \pi/K(r-a)^2 \quad (4)$$

K is a "wall correction factor" which describes the frictional resistance to diffusion within a cylindrical pore relative to that in free solution. Values of K were calculated over the range $O < a/r < 1.0$ by Paine and Scherr (from Paine et al. 1975).

The value of p_{min} calculated above is represented by line A in Fig. 7, and indicates that for molecules of about 1 nm radius the cylindrical pores need to be 2 nm radius. Plasmodesmata do not possess single cylindrical channels of that size. The desmotubule is much too small: most electron-microscopy preparations show it to have a maximum radius of between 0.5 to 0.8 nm, and some (Overall et al. 1982) suggest that the cross-sectional area of the desmotubule lumen is equivalent to but a few water molecules packed around the head groups of the membrane lipids. This leaves the cytoplasmic annulus as the most likely pathway for the movement of the molecular probes. The annulus clearly cannot be treated as a single cylindrical channel, nor can it be treated as a simple solution-filled annular passage, for there is evidence to indicate that globular particular occupy some of the volume of the annulus space. Such particles have been observed in conventionally-fixed $FeCl_3$/tannic-acid-stained preparations (Overall et al. 1982) and in fixed, freeze-fractured specimens (Thomson and Platt-Aloia 1985). Also, the fact that a desmotubule often remains in a plasmodesma despite plasmolysis (Hughes 1977) or fragmentation (Burgess 1971) indicates that it is held in place, presumably by material in the annulus. Neither the arrangement, number, nor size of particles in the annulus is known with any certainty for *Abutilon*. Nevertheless, any material in the annulus reduces

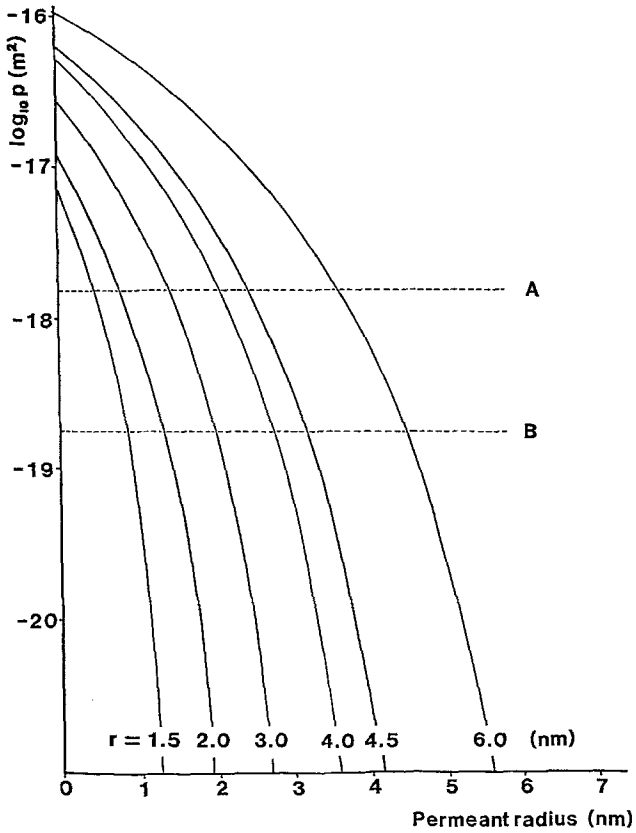

Fig. 7. Mean effective cross-sectional area for diffusion through individual cylindrical pores (p), as defined by eq. (4), plotted as a function of tracer radius, a, for several pore radii, r. Minimum values of p are marked on the graph as calculated from eqs. (1) and (3) using the minimum rate constant for diffusion as defined in the text. The value of p at A assumes one cylindrical channel per plasmodesma, e.g. the desmotubule, for the pathway for diffusion; at B the value of p assumes nine cylindrical channels per plasmodesma, which approximates for the pathway being through the cytoplasmic annulus of the plasmodesma. Curves taken from Paine et al. 1975

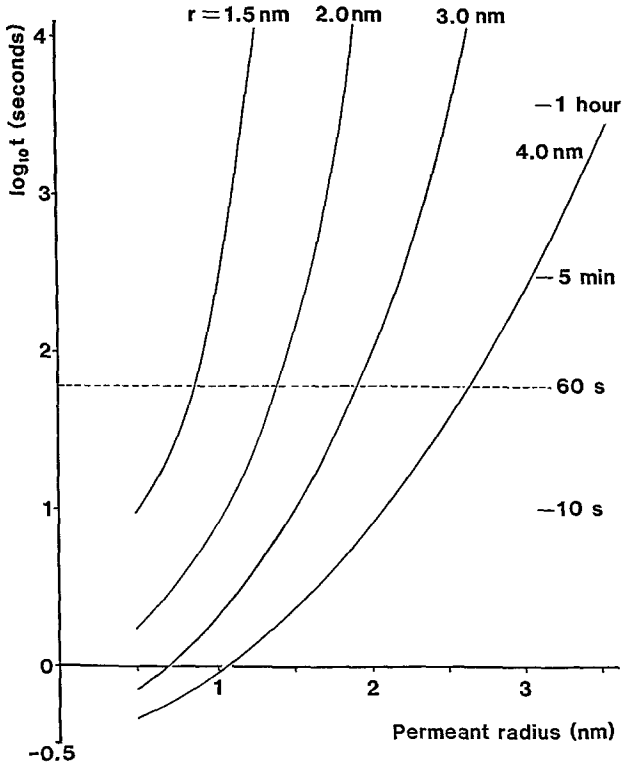

Fig. 8. Times for fluorescent probes of hydrodynamic radius a to reach the threshold of detection in the cell adjacent to the injected tip cell by diffusion through cylindrical pores of radius r, assuming nine channels per plasmodesma. These curves were constructed from values of p drawn from Fig. 7 which were used in eqn. (3) to derive values of k from which the time to minimum detection could be calculated from eqn. (1). Estimates of translational diffusion coefficients in the channels for the probes of radius a were taken from Paine et al. 1975, and ranged from $4.5 \cdot 10^{-11} \cdot m^2 \cdot s^{-1}$ for $a = 0.5$ nm to $2.0 \cdot 10^{-11} \cdot m^2 \cdot s^{-1}$ for $a = 2.5$ nm

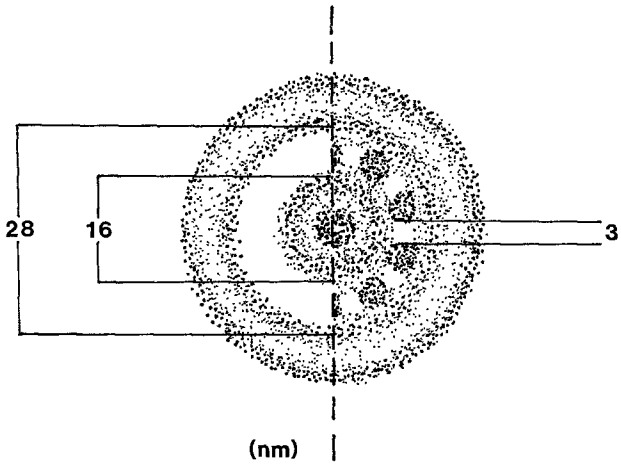

Fig. 9. Diagrammatic representation of a plasmodesma in transverse section. The average dimensions shown are for plasmodesmata in the stalk cell distal wall of mature trichomes from flowers of *Abutilon megapotamicum*, as measured from thin sections of material which had been fixed in glutaraldehyde/formaldehyde; from Hughes 1977. The cytoplasmic annulus (non-stippled area on left side of diagram) is shown with a width of 6.0 nm. The desmotubule, outer diameter 16 nm, is depicted as a tightly rolled cylinder of membrane with a virtually closed central channel. The right-hand side of the diagram shows the possible arrangement of particles and channels within the annulus: nine major particles are shown, each about 5 nm diameter, as suggested for the plasmodesmata of *Azolla* (Overall et al. 1982). The diagram does not necessarily represent the ultrastructure of plasmodesmata in living tissue

the area available for diffusion and will subdivide the pathway into a series of more or less interconnected and tortuous channels. In the plasmodesmata of *Azolla* Overall et al. (1982) think that the particles may be approximately 5 nm diameter and arranged in nine longitudinal files around the annulus, with channels between the files for longitudinal diffusion of solutes. The gap between the outer surface of the desmotubule and the inner surface of the plasmamembrane cylinder measures about 6 nm across (6 ± 2 nm, *Abutilon*, glutaraldehyde/formaldehyde/OsO_4; from Hughes 1977). If, for simplicity, the *Abutilon* annuli are considered similar to those of *Azolla* plasmodesmata, a new value of p_{min} can be calculated on the basis of nine cylindrical channels per plasmodesma. This value is represented by line B in Fig. 7 ($p_{min} = 1.754 \cdot 10^{-19}$ m^2), and corresponds to a channel radius of 1.5 nm for permeant molecules of up to 1 nm radius. Nine such channels can be easily accommodated in the annulus together with nine particles 5 nm diameter (see Fig. 9). The curves in Fig. 8 show how the time for diffusion through cylindrical channels, to the threshold of detection, is related to the radius of the permeant molecule. The curves have been drawn with values of p abstracted from Fig. 7 calculated to give values of k for nine channels per plasmodesma. Estimates for the diffusion coefficients of the different sizes of molecules have been taken from Paine et al. (1975) and other values were as for the previous calculations. Mobile dyes (e.g. F; a = 0.6–0.7 nm) generally reach the level of detection 5–10 s after injection; those that do not manage to reach the threshold of detection within 60 s are classed as non-mobile (e.g. F-Trp-Phe; $a = 0.9$ nm). If the annulus is considered to have nine distinct cylindrical channels, the results of the molecular-probe movements are best described if each channel has a radius of 1.5 nm (Table 3), and not much more or less. If $r = 2.0$ nm probes the size of F-Trp-Phe would be expected to reach the level of detection in less than 10 s. An increase in the number of channels in the annulus translates each curve in Fig. 8 vertically down the ordinate axis. Thus for each pore radius, although the maximum size of permeant which can

Table 3. Maximum values for the Stokes radii of permeants (nm) which can be expected to reach the threshold of detection within different times by diffusion through plasmodesmata having nine cylindrical pores per annulus, each of radius r

Time to detection	Pore radius r (nm)			
	1.50	2.00	3.00	4.00
10 s (Very mobile)	0.50	1.06	1.48	2.06
60 s (Mobile)	0.88	1.42	1.90	2.66
5 min (Non-mobile)	1.02	1.62	2.20	3.06

diffuse sufficiently quickly increases slightly, the rate at which an increase in permeant size decreases its apparent mobility rises dramatically – so the molecular exclusion limit becomes more sharply defined with respect to the hydrodynamic radius of the molecular probe. For instance, if there were 20 channels, each 1.5 nm radius, per plasmodesma then molecules up to 0.7 nm radius would be detected within 10 s, 1.0-nm radius molecules would need 60 s, and molecules of 1.12 nm radius would be detectable only after 5 min.

The conclusion from the calculations, given the assumptions that have been made, is that the cytoplasmic annulus is the most likely pathway for the diffusion of the molecular probes through a plasmodesma, and that the rates of diffusion observed for the different types of probe are best explained if the annular gap is considered to be divided into a number of discrete cylindrical channels, perhaps 10 to 20, each of radius of not much more or less than 1.5 nm. Such a model for the annulus is in accord with the known ultrastructure of the plasmodesmata, and the dimensions known for the annulus are more than adequate to accommodate the suggested arrangement of channels and particles (see Fig. 9). Most measurements show the gap to be substantially wider than this in the median part of a plasmodesma (Gunning and Hughes 1976; Hughes 1977; Robards 1982), but many, if not all, plasmodesmata have neck restrictions at their openings (Robards 1982) and these will be the points at which the rate of diffusion will be governed. (See Blake 1978, for analysis of the effect of the neck restrictions on volume flow rates.)

Work is in progress to establish the correlation between molecular and electrical conductivities of the plasmodesmata in the *Abutilon* trichome system. The electrical conductivity of plasmodesmata in higher plants has been estimated before by Spanswick (1972) and Overall and Gunning (1982), but not in a simple linear system of cells like that of nectary trichomes; the electrical conductivity was not correlated with molecular conductivity of the plasmodesmata. Measurement of the electrical conductivity of the plasmodesmata is expected to provide a sensitive way to study how the symplastic pathway controls the movement of relatively large molecules between cells.

We are grateful to the Agriculture and Food Research Council for the award of a grant in support of this work and to Dr. P.D. Bailey for his help and advice on the synthesis of peptides.

References

Blake, J.R. (1978) On the hydrodynamics of plasmodesmata. J Theor. Biol. **74**, 33–47

Burgess, J. (1971) Observations on structure and differentiation in plasmodesmata. Protoplasma **73**, 83–95

Clarkson, D.T., Robards, A.W. (1975) The endodermis, its structural development and physiological role. In: The Development and function of roots, pp. 425–436, Torrey, J.G., Clarkson, D.T., eds. Academic Press, London

Erwee, M.G., Goodwin, P.B. (1983) Characterisation of the *Egeria densa* Planch. leaf symplast: inhibition of the intercellular movement of fluorescent probes by group II ions. Planta **158**, 320–328

Erwee, M.G., Goodwin, P.B. (1984) Characterisation of the *Egeria densa* leaf symplast: response to plasmolysis, deplasmolysis and to aromatic amino acids. Protoplasma **122**, 162–168

Erwee, M.G., Goodwin, P. (1985) Symplast domains in extrastelar tissues of *Egeria densa* Planch. Planta **163**, 9–19

Findlay, N., Mercer, F.V. (1971a) Nectar production in *Abutilon*. 1 – Movement of nectar through the cuticle. Aust. J. Biol. Sci. **24**, 647–656

Findlay, N., Mercer, F.V. (1971b) Nectar production in *Abutilon*. 2– Sub-microscopic structure of the nectary. Aust. J. Biol. Sci. **24**, 657–664

Findlay, N., Reed, M., Mercer, F.V. (1971) Nectar production in *Abutilon*. 3 – Sugar secretion. Aust. J. Biol. Sci. **24**, 665–675

Goodwin, P.B. (1983) Molecular size limit for movement in the symplast of the *Elodea* leaf. Planta **157**, 124–130

Goodwin, P.B., Erwee, M.G. (1985) Intercellular transport studied by micro-injection. In: Botanical microscopy 1985, pp. 335–358, Robards, A.W., ed. Oxford University Press, Oxford

Granath, K.A., Kvist, B.E. (1967) Molecular weight distribution analysis by gel chromatography on Sephadex. J Chromatogr. **28**, 69–81

Gunning, B.E.S., Hughes, J.E. (1976) Quantitative assessment of symplastic transport of pre-nectar into trichomes of *Abutilon* nectaries. Aust. J. Plant Physiol. **3**, 619–637

Gunning, B.E.S., Robards, A.W. (1976a) Intercellular communication in plants: studies on plasmodesmata. Springer, Heidelberg

Gunning, B.E.S., Robards, A.W. (1976b) Plasmodesmata: current knowledge and outstanding problems. In: Intercellular communication in plants: studies on plasmodesmata, pp. 297–311, Gunning, B.E.S., Robards, A.W., eds. Springer, Heidelberg

Hughes, J.E. (1977) Aspects of ultrastructure and function in *Abutilon* nectaries. M.Sc. Thesis, Australian National University, Canberra, ACT

Kronestedt, E.C., Robards, A.W., Stark, M., Olesen, P. (1986) Development of trichomes in the *Abutilon* nectary gland. Nordic J. Bot. **6**, 627–639

Merrifield, R.B. (1964) Solid-phase peptide synthesis. III. An improved synthesis of Bradykinin. Biochemistry **3**, 1385–1390

Olesen, P. (1979) The neck constriction in plasmodesmata: evidence for a peripheral sphincter-like structure revealed by fixation with tannic acid. Planta **144**, 349–358

Overall, R.L., Wolfe, J., Gunning, B.E.S. (1982) Intercellular communication in *Azolla* roots. I. Ultrastructure of plasmodesmata. Protoplasma **111**, 134–150

Overall, R.L., Gunning, B.E.S. (1982) Intercellular communication in *Azolla* roots: II. Electrical coupling. Protoplasma **111**, 151–160

Paine, P.L., Moore, L.C., Horowitz, S.B. (1975) Nuclear envelope permeability. Nature **254**, 109–114

Pitts, J.D., Finbow, M.E. (1982) The functional integration of cells in animal cells. Cambridge University Press, Cambridge

Reed, M.L., Findlay, N., Mercer, F.V. (1971) Nectar production in *Abutilon*. 4-Water and solute relations. Aust. J. Biol. Sci. **24**, 677–688

Robards, A.W. (1975) Plasmodesmata. Annu Rev. Plant Physiol. **26**, 13–29

Robards, A.W. (1982) Cell interactions in plants – a comparative study. In: Functional integration of cells in animal tissues (British Society for Cell Biology Symp.) pp. 57–79, Pitts, J.D., Finbow, M.E., eds. Cambridge University Press, Cambridge

Rose, G.D., Geselowitz, A.R., Lesser, G.J., Lee, R.H., Zehfus, M.H. (1985) Hydrophobicity of amino acid residues in globular proteins. Science **229**, 834–838

Simpson, I. (1978) Labelling of small molecules with fluorescein. Anal. Biochem. **89**, 304–305

Spanswick, R.M. (1972) Electrical coupling between cells of higher plants: a direct demonstration of intercellular communication. Planta **102**, 215–227

Thomson, W.W., Platt-Aloia, K. (1985) The ultrastructure of the plasmodesmata of the salt glands of *Tamarix* as revealed by transmission and freeze-fracture electron microscopy. Protoplasma **125**, 13–23

Tucker, E.B. (1982) Translocation in the staminal hair of *Setcreasa purpurea*. I. A study of cell ultrastructure and cell to cell passage of molecular probes. Protoplasma **113**, 193–202

Tucker, E.B., Spanswick, R.M. (1985) Translocation in the staminal hairs of *Setcreasea purpurea*. II/Kinetics of intercellular transport. Protoplasma. **128**, 167–172

Received 4 September 1986; accepted 22 January 1987